Research Article

Design, synthesis and anti-diabetic activity of some novel xanthone derivatives targeting α-glucosidase

Design, synthesis and anti-diabetic activity of some novel xanthone derivatives targeting α-glucosidase

Partha Sarathi Bairy[1], Aparoop Das[1], Lalit Mohan Nainwal[1], Tapan Kumar Mohanta[2], Mukesh Kumar Kumawat[3], Pradyumna Kishore Mohapatra[3] and Pratap Parida[4]

[1]Department of Pharmaceutical Sciences, Dibrugarh University, Dibrugarh, Assam 786 004, India; [2]Free Major of Natural Science, School of Basic Studies, Yeungnam University, 280, Daehak Gyeongsan, Gyeongsanbuk, 712-749, Republic of Korea ; [3]Anand College of Pharmacy, Keetham, Agra, Uttar Pradesh 282 007, India; [4]Regional Medical Research Centre, NE Region, Indian Council of Medical Research, Dibrugarh, 786 001, Assam, India.

Abstract

Twenty eight xanthone derivatives were designed and docked into the N-terminal catalytic domain of maltase-glucoamylase (ntMGAM) by considering miglitol as standard drug. Most of the molecules showed excellent docking scores and docking interaction as compared to the binding cavity of the standard molecule. The five best scoring ligands were synthesized and characterized by a number of analytical and spectroscopic techniques. The molecules were screened for the *in vivo* anti-diabetic activity in streptozotocin-induced diabetic animal model in Wistar rats. Compound P4 showed the most prominent inhibition among others. The synthesized compounds reported significant (p<0.01) effect in lowering blood glucose levels compared to miglitol as a standard α-glucosidase inhibitor.

Introduction

Glucosidase catalyzes especially hydrolyses the carbo-hydrates to free glucose unit in blood in the final step of carbohydrate metabolism. Glucosidase causes hydro-lysis of α and β glycosidic linkages of carbohydrates, thus they are α-glucosidase and β-glucosidase (Height-man et al., 1999). Among them α-glucosidase (EC 3.2.1.20) draws considerable interest to the pharmaceu-tical research community because it helps to increase postprandial blood glucose level (Park et al., 2008). Inhibition of the enzyme is a useful chemotherapy for controlling diabetes and obesity. Due to its catalytic role, it also targeted in the treatment of other carbo-hydrate mediated diseases, including cancer (Hum-phries et al., 1986), viral infections (Mehta et al., 1998; Karpas et al., 1988), and hepatitis (Zitzmann et al., 1999).

Since the discovery of acarbose, first α-glucosidase

inhibitor lots of synthetic (Xu et al., 2007; Tanabe et al., 2007; Liu et al., 2007) and natural molecules (Luo et al., 2007; Saludes et al., 2007; Du et al., 2006) reported for the management of type 2 diabetes, but continuous administration of these agents causing adverse effects like diarrhea, abdominal discomfort, flatulence (Cam-pbell et al., 2000), and hepatotoxicity (Hsiao et al., 2006).

So, the research continues to find other problem solving alternatives. Several fields of research upon xanthone nucleus going on and recent studies indicate that man-giferin, a xanthone C-glycoside, serve as potent α-glucosidase inhibitors (Liu et al., 2006).

Xanthones are secondary metabolites found in plants, fungi and lichens and now in the center of research interest by the past two decades because of its diverse class of pharmacological profile (Cardona et al., 1990). Xanthones are reported for biological activities like anti-tumor, anti-oxidant, anti-inflammatory, anti-allergy,

anti-bacterial, antifungal, antiviral (Diderot et al., 2006), antimycobacterial (Pickert et al., 1998), antidepressant (Galt et al., 1989), anti-diabetic (Liu et al., 2006) and monoamine oxidase inhibitors.

Materials and Methods

Design of new molecules

A xanthone nucleus with different substitutions is proved to have a diverse class of pharmacological profile. Previously established α-glucosidase inhibitor like acarbose, miglitol were observed to have polyhydroxy groups in their structure and new molecules are designed considering this fact. For this study, xanthones with several hydroxy groups and alkoxy groups at different position are designed and drawn using ChemAxon, a freeware developed by Advanced Chemistry Development, Inc. and converting 2D chemical structure of compound to 3D structures (Nainwal et al., 2014).

Molecular property

All the drawn structures were screened for *in silico* biological data prediction using Molinspiration online filter and Drulito software. They screened the designed molecules according to 'Lipinski's rule of five' predicting molecular properties like molecular weight, total polar surface area (TPSA), LogP, hydrogen bond donor (HBD), hydrogen bond acceptor (HBA) and number of roratable bonds.

Drug likeness and bioavailability

Virtual screening of the compounds was performed before molecular docking simulation studies. All the compounds were screened for predictive molecular physicochemical properties such as absorption, distribution, metabolism, excretion and toxicity (ADME/Tox). This aids the screening of the compounds for potential drug like properties. Drug intensity and kinetics of drug contact to various tissues is greatly influenced by ADME/Tox, which in turn reflects the efficiency and pharmacological activity of the compound as a drug. The mutagenicity, tumourogenicity, irritating and reproductive effects as well as drug likeness and drug scores of the compounds were predicted by using OSIRIS property explorer (http://www.organic-chemistry.org/prog/peo/).

Protein retrieval and preparation

α-Glucosidase crystal structure was obtained from RCSB (Research Collaboratory for Structural Bioinformatics), Protein Databank (PDB, http://www.pdb.org). The PDB ID of the selected protein was found to be 3L4W (Sim et al., 2010) and downloaded as PDB text file format. All the heteroatom including co-crystallized ligand was removed by Molegro Molecular Viewer to make protein free and suitable for further docking studies. Now the protein comprises of only one chain containing 863 amino acid residues and 13493 numbers of atoms and 13693 numbers of bonds. Additions of nonpolar hydrogens were done for better interaction. Kollman united atom charges were applied to the protein. Appropriate ionization and tautomeric states of numerous amino acid residues such as Arg, His, Asp, Glu and Ser were managed by adding H-atoms to the protein at pH 7.0.

Molecular docking study

Molecular docking is generally used to detect the protein-ligand orientation and interaction. AutoDock Tools package version 2.4 was utilized to create the docking input files. The grid region was surrounded by the active site for binding. So, grid region was selected on the basis of amino acid residues representing the binding site of miglitol as the standard drug obtained from PDB with ID- 3L4W and considered as the best active region for the favorable interaction. The grid box was set at 80 × 80 × 80 A° for x, y and z axis and covered 12 amino acid residues (TYR299, ASP327, ILE364, TRP406, TRP441, ASP443, MET444, ARG526, TRP539, ASP542, PHE575, HIS600) of active site. The Lamarckian Genetic Algorithm (LGA), a local search algorithm was utilized for ligands conformers searching. During the docking process, a maximum of 10 conformers were considered for each compound. This method was applied for each designed compound and after completion the conformer with lowest binding energy was chosen.

The conformational similarity by visualizing the binding site and its energy (Kcal/mol), and the docked amino acid residues forming hydrogen bonds and other parameters like intermolecular energy (Kcal/mol) and inhibition constant (µM) were analyzed by AutoDock tool. Ten best poses were generated for each ligand and scored using AutoDock 4.2 scoring functions (Morris et al., 1998). Based on the docked energy all the ligands were ranked. The ligand interacting residues with the target protein were analyzed using AutoDock tools, PyMOL (Konc et al., 2011) and LigPlot (Madeswaran et al., 2011).

Chemistry

Structural investigation

All chemicals used in the work were used without further purification. The intermediate was taken in an open capillary on the Veego-MPI melting point apparatus and the melting point of the synthesized compounds was determined. The progress of the reactions was monitored on silica gel-G TLC plate using various solvent combinations. The spots were detected with iodine vapors and observed under UV-light. The UV–visible spectra of the synthesized compounds were

recorded on UV–visible spectrophotometer (*Shimadzu UV*-1800). Infrared spectra were recorded on an FT-IR Perkin-Elmer spectrometer. The ^{1}H and ^{13}C NMR spectra were recorded at 400 MHz and 100 MHz, respectively, on a *Bruker Avance-II* 400 NMR spectrometer using DMSO-d_6 as solvent with tetramethylsilane (TMS) as an internal standard. Mass spectra were obtained on a Waters Q-TOF MICROMA SS LC mass spectrometer (Silverstein and Webster, 1963).

General procedure

Salicylic acid derivative and polyhydroxy phenols were used to synthesize hydroxyxanthones (intermediate) and further alkylation done by various alkyl bromide in the presence of acetone (Scheme 1). For the synthesis of hydroxyxanthones Eaton's reagent (Eaton and Carlson, 1973) was poured in the mixture of salicylic acid derivative (60 mmol) and polyhydroxy phenol (60 mmol), stirred at 70°C for 30 min. The mixture cooled, stirred with cold water, keeping temperature 0-4°C for 2.5 hours. The resulting solid collected by filtration, washed with water until pH 6 and dried at 60°C (Varache-Lembege et al., 2008). To the intermediate (2 mmol) and alkyl bromide (3 mmol) in acetone (55-60 mL) was added potassium carbonate (2.5 mmol). Mixture was refluxed under stirring for 2-4 hours, cooled, filtered and it concentrated. Further recrystallization was done and the product collected as yellow solid (Liu et al., 2006).

3-butoxy-9H-xanthene-9-one, P10

Yellow color solid; %Yield 65.3; M.P. 237-238°C; Spectroscopic analysis: λ_{max} (Acetone): 542; FTIR (cm^{-1}): 2880.73 (C-H$_{stret}$), 1597.83 (C=C Ar$_{stret}$), 1643.72 (C=O$_{stret}$, keto group), 1144.77 (C-O$_{stret}$, six member cyclic ether); ^{1}H NMR (400MHz, DMSOd$_6$, δ in ppm): 2.485-2.513(m, 9H, Aliphatic -CH$_2$), 7.151-7.181 (m, 7H, =C-H, Ar); ^{13}C NMR (100 MHz, DMSOd$_6$, δ in ppm): 38.99, 39.15, 39.51, 39.85, 115.74, 116.14, 120.36, 130.12, 131.47, 162.51, 172.21; MASS (m/z): 252.84 (M$^+$)

3,6-dipropoxy-9H-xanthene-9-one, P22

Brownish yellow solid; %Yield 78.8; M.P. 247-249°C; Spectroscopic analysis: λ_{max} (Acetone) 544; FTIR (cm^{-1}): 2854.64 (C-H$_{Stret}$), 1541.39 (C=C Ar$_{Stret}$), 1715.55 (C=O$_{Stret}$, keto group), 1096.96 (C-O$_{Stret}$, six member cyclic ether); ^{1}H NMR (400 MHz, DMSOd$_6$, δ in ppm): 3.2147-3.322 (m, 18H, Aliphatic -CH$_2$), 7.181-7.205 (m, 6H, =C-H, Ar); ^{13}C NMR (100 MHz, DMSOd$_6$, δ in ppm): 38.83, 39.03, 39.24, 39.45, 39.66, 39.87, 40.08, 78.42, 78.75, 78.95, 102.78, 108.14, 113.64, 133.39, 161.68, 165.50; MASS (m/z): 316.032 (M$^+$)

1-hydroxy-3-methoxy-9H-xanthene-9-one, P2

Yellow color solid; %Yield 63.4; M.P. 232-234°C; Spectroscopic analysis: λ_{max} (Acetone) 544; FTIR (cm^{-1}): 2876.95, 2973.44 (C-H$_{Stret}$), 1556.75 (C=C Ar$_{Stret}$), 1733.06 (C=O$_{Stret}$, keto group), 1044.91 (C-O$_{Stret}$, six member cyclic ether), 1419.00 (C-H$_{bend}$); ^{1}H NMR (400 MHz, DMSOd$_6$, δ in ppm): 2.511 (s, 3H, –CH$_3$), 2.527 (s, 1H, –OH), 7.525-7.545 (m, 6H, =C-H, Ar); ^{13}C NMR (400 MHz, DMSOd$_6$, δ in ppm): 38.82, 39.02, 39.44, 40.07, 62.99, 64.16, 72.40, 78.47, 79.01, 79.13, 92.90, 97.30, 103.06, 115.66, 116.24, 117.54, 119.87, 120.16, 124.18, 125.00, 130.11, 131.39, 135.50, 155.42, 157.28, 162.29, 165.82, 172.46; MASS (m/z): 252.956 (M$^+$)

1-hydroxy-3-propoxy-9H-xanthene-9-one, P4

Light yellow solid; % Yield 77; M.P. 240-243°C; Spectroscopic analysis: λ_{max} (Acetone) 556; FTIR (cm^{-1}): 2885.44 (C-H$_{Stret}$), 1539.96 (C=C Ar$_{Stret}$), 1748.21 (C=O$_{Stret}$, keto group), 1138.03 (C-O$_{Stret}$, six member cyclic ether), 1388.86 (C-H$_{bend}$); ^{1}H NMR (400 MHz, DMSOd$_6$, δ in ppm): 2.454 (m, 7H, aliphatic –CH$_2$), -2.512(s, 1H, –OH), 7.733-7.757(m, 6H, =C-H, Ar); ^{13}C NMR (400 MHz) DMSOd$_6$, δ(ppm): 38.77, 38.97, 39.18, 39.60, 39.81, 40.02, 115.75, 116.14, 120.37, 130.07, 131.44, 162.55, 172.08; MASS (m/z): 309.043 (M$^+$)

3-butoxy-1-hydroxy-9H-xanthene-9-one, P5

Greyish yellow solid; %Yield 72.6; M.P. 239-241°C;
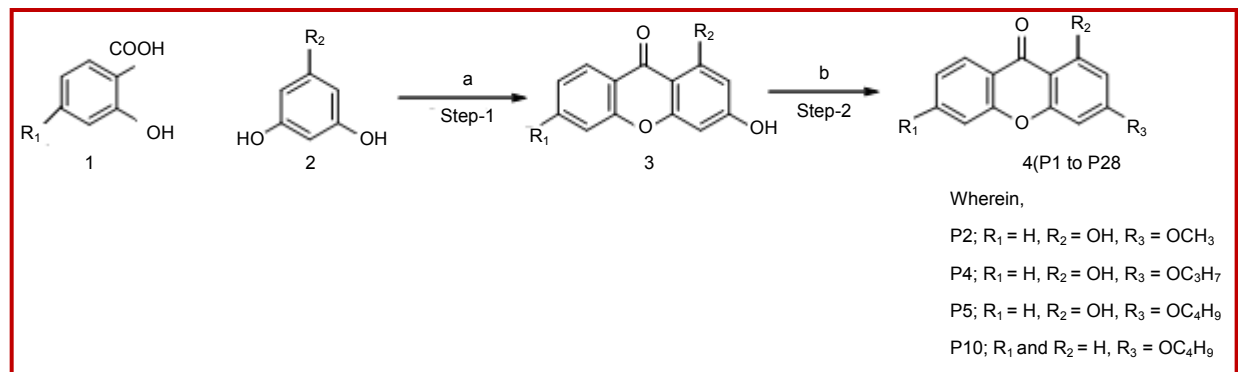
Scheme 1: Synthesis of alkoxyxanthones; Reagents and conditions: (a) Stirring with Eaton's reagent at 70°C for 35 min; then at 0-5°C for a further 2 hours 30 min (b) RBr, Acetone, K$_2$CO$_3$, Reflux for 4 hours at 55°C

Spectroscopic analysis: λ_{max} (Acetone) 542; FTIR (cm^{-1}): 2971.00,2880.73 (C-H$_{Stret}$), 1541.07 (C=C Ar$_{Stret}$), 1732.14 (C=O$_{Stret}$, keto group), 1145.77 (C-O$_{Stret.}$, six member cyclic ether), 1373.22 (C-H$_{bend}$); ^{1}H NMR (400 MHz, DMSOd$_{6}$, δ in ppm): 2.5232(m, 7H, aliphatic –CH$_2$), 2.612(s, 1H, –OH), 8.147-8.171 (m, 6H, =C-H, Ar); ^{13}C NMR (400 MHz, DMSOd$_{6}$, δ in ppm): 30.42, 38.86, 39.28, 39.69, 39.90, 40.11, 68.16, 78.52, 78.85, 79.06, 79.18, 92.91, 97.37, 115.66, 116.11, 117.55, 120.28, 124.21, 125.24, 130.06, 131.31, 135.52, 162.43, 166.01, 172.30; MASS (m/z): 285.067 (M^{+})

Evaluation of anti-diabetic activity

Synthesized compounds are evaluated for *in vivo* anti-diabetic activity in diabetic rats using streptozotocin as diabetic inducing agent (Abeeleh et al., 2009).

Animals

Adult male Wistar rats (150–200 g) were used to study the anti-diabetic activity. Animals were housed in standard laboratory conditions (temperature 22 ± 2°C and humidity 45 ± 5% with 12 hours day: 12 hours night cycle). All animals received standard laboratory diet and water *ad libitum*.

Acute toxicity studies

Acute oral toxicity study was performed according to OECD-423 guidelines (acute toxic class method). Adult female Wistar rats (n = 5; 120-200 g) were selected by random sampling for acute toxicity study. The animals were kept fasting overnight and provided water *ad libitum*. The synthesized drugs were administrated orally at 5 mg/kg body weight orally and observed for 14 days. If mortality was observed in two out of three animals, then the dose administrated was assigned as toxic dose. If mortality was observed in one animal, then the same dose repeated again to confirm the toxic dose. If mortality was not observed, the procedure was repeated for higher doses such as 50, 100 and 1500 mg/kg body weight. Animals were observed individually after dosing for first 30 min, 1 hour, 2 hours and daily thereafter, till 14 days. Any toxicity sign of gross changes in skin and fur, eyes and mucous membranes, circulatory, respiratory, autonomic and central nervous systems, and behavior pattern was reported (Kumudhavalli and Jaykar, 2012).

Induction of diabetes

Type 2 diabetes mellitus was induced by injecting freshly prepared streptozotocin (50 mg/kg; i.p.) in cold citrate buffer (0.1M, pH 4.5) (Ramachandan et al., 2013) in overnight fasting experimental rats. Confirmation of diabetes was decided to measure blood glucose level after 72 hours of injecting streptozotocin. Each time blood from tail vein of experimental rats is collected and blood glucose was measured with glucometer

during whole study. Animals were kept in laboratory condition for 7 day to stabilize diabetes and animals showing blood glucose >250 mg/dL taken for activity assessment of synthesized drugs.

Study design and grouping of animals

Animals were randomly divided into 13 groups (n = 5) for the whole study. 1st group treated as normal control and administered 0.3% carboxymethyl cellulose (CMC). 2nd group remains diabetic control and no drug administered throughout the study period. Standard drug (miglitol) at a dose level of 25 mg/kg (p.o.) body weight was administered to 3rd group. Others groups receive synthesized drugs of two dose level i.e. 100 mg/kg and 250 mg/kg body weight. All the drugs were suspended on freshly prepared CMC (0.3% w/v) before administered. The treatments were administered orally to the animals daily for 14 days. Blood samples were collected from tail vein for determination of blood glucose level on 0, 5th, 10th and 15th day (Selvan et al., 2008). The blood glucose levels were measured by one touch glucometer (AccuSure) throughout the two weeks of treatment.

Body weight measurement

Animals were weighed on 0, 5th, 10th and 15th day after treatment to detect any change in their body weights.

Blood sample collection

On 15th day blood samples were collected from retro-orbital puncture under mild anesthesia and stored with 4%w/v sodium citrate for plasma separation. The animals were sacrificed through cervical dislocation after subjecting them to mild ether anesthesia. Blood was carefully collected from each rat from retro-orbital puncture under mild anesthesia in microfuge tube and then centrifuged at 2,500 rpm for 15 min. Plasma, thus obtained, was collected carefully in individual micro-fuge tube and stored at –20°C. Plasma was separated immediately and used for the analysis of total cholesterol (TC) and triglyceride (TG).

Biochemical estimation

Serum marker such as serum glutamic oxaloacetic transaminase (SGOT), serum glutamic pyruvic trans-aminase (SGPT) and alkaline phosphatase (ALP) were measured (Cole et al., 2005; Silverstein and Webster, 1963). Lipid profile like triglyceride and total cholesterol were also measured using test kits.

Statistical analysis

All the data were expressed as mean ± SEM. Statistical analysis was carried out by one way ANOVA (Analysis of Variance) followed by Dunnett's t-test with the level of significance at p<0.01 and p<0.05.

Results

Drug likeness studies

The compounds were derived from the xanthone nucleus with various substituents (Table I). Pharmacokinetics properties and toxicity studies of all the derived compounds were studied. Molecular properties

Table I			
Molecular docking results			
SL. No.	Ligand code	Substitution	Binding energy
1	P1	1-OH, 3-OH	-9.19
2	P2	1-OH, 3-OCH$_3$	-10.20
3	P3	1-OH, 3-OC$_2$H$_5$	-9.78
4	P4	1-OH, 3-OC$_3$H$_7$	-9.89
5	P5	1-OH, 3-OC$_4$H$_9$	-9.99
6	P6	3-OH	-8.66
7	P7	3-OCH$_3$	-9.72
8	P8	3-OC$_2$H$_5$	-9.25
9	P9	3-OC$_3$H$_7$	-9.68
10	P10	3-OC$_4$H$_9$	-9.93
11	P11	3-OH, 6-OH, 8-OH	-7.93
12	P12	1-OH, 3-OH, 6-OH	-8.37
13	P13	1-OH, 3-OH, 6-OH, 8-OH	-8.61
14	P14	5-OH, 7-OH	-7.39
15	P15	1-OH, 4-OH	-8.12
16	P16	3-OH, 8-OH	-8.08
17	P17	1-OH, 5-OH	-8.06
18	P18	3-OH, 6-OH, 7-OH	-7.65
19	P19	3-OH, 6-OH	-9.5
20	P20	3,6-OCH$_3$	-10.08
21	P21	3,6-OC$_2$H$_5$	-9.16
22	P22	3,6-OC$_3$H$_7$	-12.99
23	P23	3,6-OC$_4$H$_9$	-8.98
24	P24	2-OC$_2$H$_5$	-9.08
25	P25	5-OC$_2$H$_5$	-9.14
26	P26	6-OC$_2$H$_5$	-7.17
27	P27	3-OCOCH$_3$	-8.83
28	P28	3-OCOC$_2$H$_5$	-9.16

of the designed ligands such as logP, molecular weight, HBA (hydrogen bond acceptor), HBD (hydrogen bond donor), nRB (number of rotatable bond), TPSA (total polar surface area) were calculated by Molinspiration property calculator and are reported in Table II. Most of the compounds showed good predictive bioavailability and pharmacokinetics hardly violating the Lipinski rule. The ligands were further studied for different property such as mutagenicity, tumourogenicity, irritating and reproductive effects as well as drug likeness and drug scores and were predicted.

Docking study

Prior to the docking simulation, the authors were applied the re-docking process to validate the docking protocol for its reproducibility. The co-crystal migiltol docked into the binding pocket of human maltase-glucoamylase. The structural superimposition of the crystal ligand along with the crystal ligand was perfomed by AutoDock 4.2. The docked pose of Migiltol achieved by AutoDock and the co-crystal conformation results an RMSD of 1.33 Å (Figure 1). The RMSD of <2 Å were considered as success wherever the RMSD between 2 and 3 Å were believed to be partially successful. It was found that all the interactions and interacting residues in the docked pose were identical with the co-crystal ligand. Lowest RMSD value, similar interactions and binding poses with same interacting residues between the docked ligand and the crystal ligand validates our docking protocol to be optimal. The molecules were targeted to the binding site of the standard compound. The docking results predicted that migiltol had less binding affinity as compared to the most of the derived compounds.

Docking results were predicted that the standard ligand had a -8.71 Kcal/mol binding energy. The hydrogen bond forming amino acid residues of the target protein was found to be Asp327, Trp406, Asp443 and Met444. Excluding hydrogen interaction, the ligand was also formed nine hydrophobic bonds with the amino acids (Figure 2). The ligand p22 was predicted to have better binding energy as compared to the standard drug. It formed a -12.99 Kcal/mol binding energy. It only formed seven hydrophobic bonds with the target protein to the same binding pattern as of the standard (Figure 3). Docking interaction of the ligand p2 was formed -10.2 Kcal/mol binding energy. Two hydrogen bond interactions were identified with the amino acid residue Trp406 and Arg526. It also formed twelve hydrophobic interactions with the protein. The ligand p5 was formed a -9.99 Kcal/mol binding energy. It was fitted to the binding pocket of the standard molecule forming ten hydrophobic interactions. The ligand p10 was inhibited the protein having binding energy -9.93 Kcal/mol. The hydrogen bond interactions were identified with the helix of protein. Two hydrogen bonds were formed by the ligand with the residue Tyr299 and

|							
Table II							
Molecular properties of the designed ligands							
S N.	Ligand code	Log P	TPSA	MW	Violations	Rotatable bonds	HBA	HBD
1	P1	2.776	70.667	228.203	0	0	4	0
2	P2	3.312	59.673	242.23	0	1	4	0
3	P3	3.688	59.673	256.257	0	2	4	0
4	P4	4.19	59.673	270.284	0	3	4	0
5	P5	4.749	59.673	284.311	0	4	4	0
6	P6	3.067	50.439	212.204	0	0	3	0
7	P7	3.603	39.445	226.231	0	1	4	0
8	P8	3.979	39.445	240.258	0	2	4	0
9	P9	4.481	39.445	254.285	0	3	4	0
10	P10	5.041	39.445	268.312	0	4	4	0
11	P11	2	90.895	244.202	0	0	5	0
12	P12	2.273	90.895	244.202	0	0	5	0
13	P13	1.981	111.123	260.201	0	0	6	0
14	P14	2.776	70.667	228.203	0	0	4	0
15	P15	3.036	70.667	228.203	0	0	4	0
16	P16	2.8	70.667	228.203	0	0	4	0
17	P17	3.036	70.667	228.203	0	0	4	0
18	P18	2.8	70.667	228.203	0	0	4	0
19	P19	2.564	70.667	228.203	0	0	4	0
20	P20	3.636	48.679	256.257	0	2	4	0
21	P21	4.388	48.679	284.311	0	4	4	0
22	P22	5.393	48.679	312.365	1	6	4	0
23	P23	6.511	48.679	340.419	1	8	4	0
24	P24	3.979	39.445	240.258	0	2	3	0
25	P25	3.955	39.445	240.258	0	2	3	0
26	P26	3.979	39.445	240.258	0	2	3	0
27	P27	3.098	56.516	254.241	0	2	4	0
28	P28	2.776	70.667	228.203	0	0	4	0
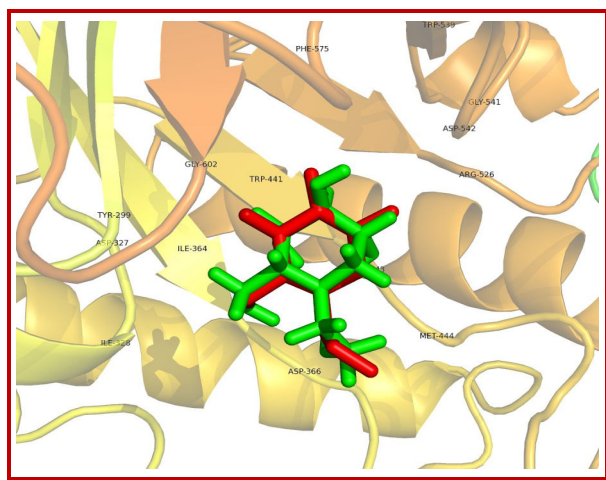
Figure 1: The re-docking pose of miglitol crystal ligand. The crystal ligand is marked in red color

Arg526. The number of hydrophobic interacting residues was found to be ten. The ligand p4 was formed -9.89 Kcal/mol binding interaction energy. It was inhibited the target protein with eight hydrophobic bonds.

Chemistry

Five best scoring (lesser binding energy) compounds (P2, P4, P5, P10 and P22) were selected for synthesis. The synthesis of selected novel alkoxyxanthones was achieved in two step reaction (Scheme 1). In the first step, salicylic acid derivative (**1**) and poly-hydroxy phenols (**2**) were reacted together to yield hydroxy-xanthones (**3**) in the presence of acid. Hydroxyxan-thones (**3**) was further reacted with alkyl bromide in the presence potassium carbonate, acetone and reflux for 4 hours at 55°C to yield targeted alkoxyxanthones (**4**).

The structures of the synthesized compounds were confirmed by various spectropic techniques viz., FT-IR spectra showed the stretching in the frequency range between regions 2853-2971 cm^{-1} due to aliphatic C-H. Whereas, the occurrence of stretching band in between 1643-1748 confirmed the presence of C = O group. The other stretching bands in 1539-1597 cm^{-1} attributable to aromatic C = C, 1044-1145 cm^{-1} due to C-O stretching of
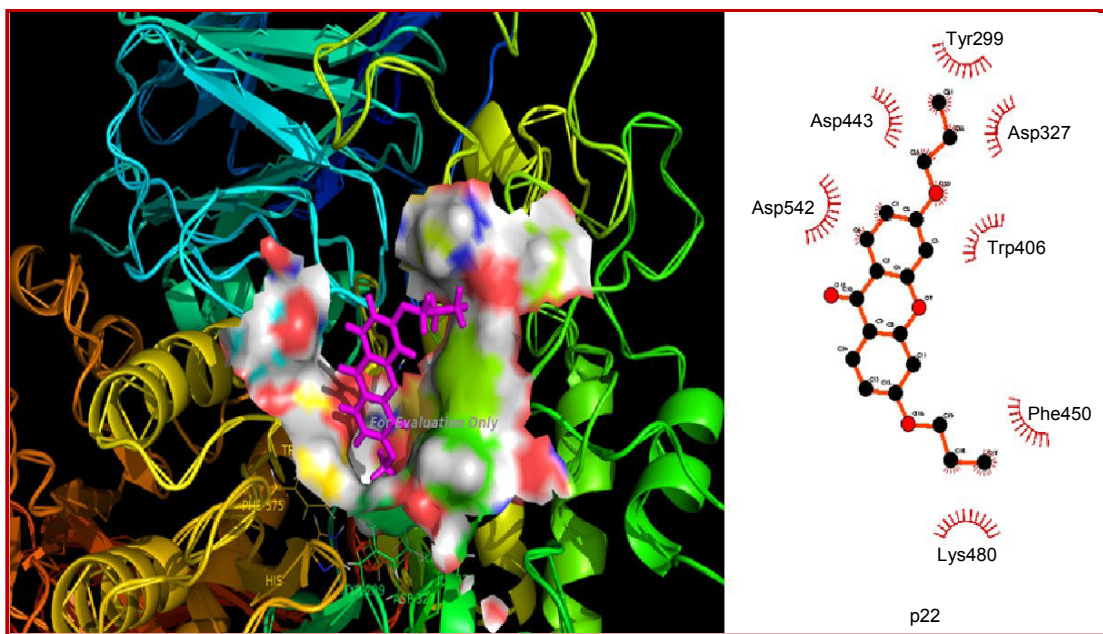
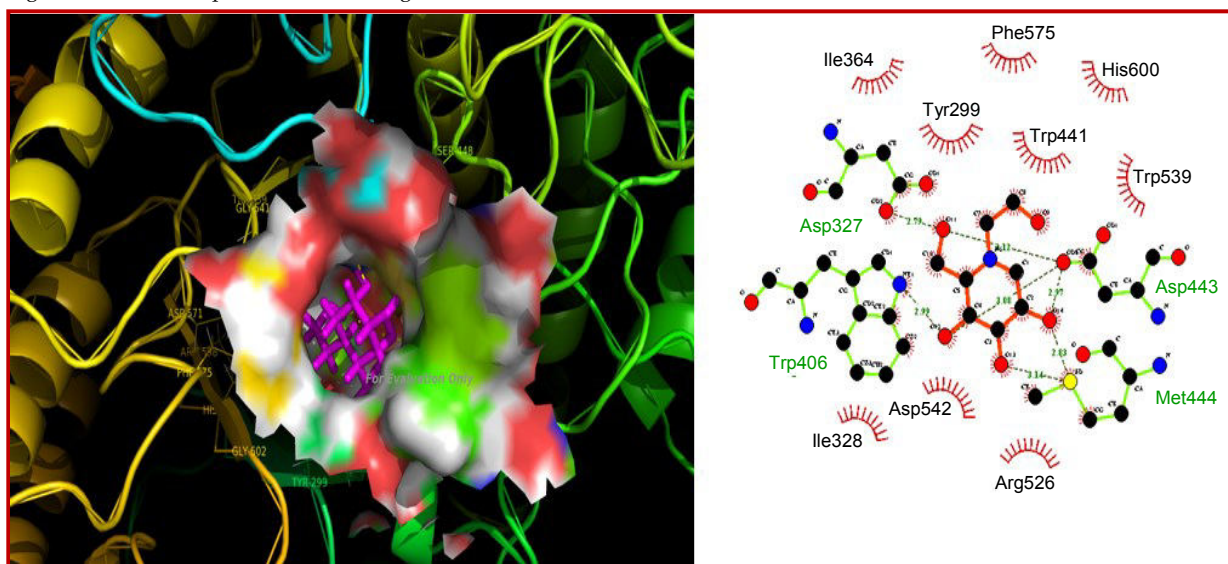Figure 2: The docked pose of standard miglitol

Figure 3: The docked pose of P22

six member cyclic ether moiety. The ^{1}H NMR spectra of the compounds showed the occurrence of various singlet, doublet, triplet or multiplet at δ (ppm) 2.50-3.52 to aliphatic –C-H and 7.18-8.20 to aromatic = C-H, further confirmed the formation of this class of derivatives.

Anti-diabetic activity evaluation

In vivo acute toxicity studies

The synthesized compounds showed no serious toxicity up to dose level 1,500 mg/kg body weight in experimental rats.

Blood glucose level

Before starting the treatments, blood glucose level of all the animals was within normal range. After 72 hours of streptozotocin treatment, the blood glucose level was significantly changed more than 240 mg/dL. There was significant decrease ($p < 0.01$) in blood glucose level of the animals after treatment with drugs on 5th day, 10th day and 15th day (Table III).

Body weight

Statistical analysis revealed that there was significant ($p < 0.01$) difference in body weight of experimental animals, among the group at 5th day, 10th day and 15th day when compared with normal control group. But there are no significant changes in body weight between the groups when compared with diabetic

Table III					
Effect on blood glucose level of synthesized compounds					
Group	Dose level (mg/kg, p.o.)	Blood glucose level on			
		0 day	5th day	10th day	15th day
Normal control	0.3% CMC	91 ± 0.4	102 ± 0.5	102.6 ± 1.1	96.4 ± 0.7
Diabetic control		242.6 ± 1.1	264.8 ± 1.5	270 ± 2.3	270 ± 0.5
Standard (miglitol)	25	286.6 ± 7.4	228.26 ± 7.2^{c}	181.0 ± 6.0^{ac}	121.7 ± 6.7^{ac}
P22	100	273.4 ± 14.1	228.8 ± 10.1^{c}	182.9 ± 12.8^{ac}	131.3 ± 6.3^{ac}
	250	285.4 ± 6.0	232.4 ± 7.7^{c}	182.0 ± 11.8^{ac}	136.4 ± 8.3^{ac}
P10	100	283.9 ± 15.9	228.9 ± 13.7^{c}	167.8 ± 9.9^{ac}	133.5 ± 5.9^{ac}
	250	275.4 ± 7.6	220.7 ± 6.3^{c}	181.0 ± 6.0^{ac}	133.3 ± 4.6^{ac}
P2	100	275.5 ± 9.5	232.0 ± 9.4^{c}	179.7 ± 10.0^{ac}	127.8 ± 10.2^{ad}
	250	278.2 ± 7.5	231.2 ± 7.4^{c}	177.0 ± 5.2^{ac}	129.7 ± 8.3^{ad}
P4	100	255.9 ± 8.8	222 ± 5.1^{c}	173.0 ± 7.7^{ac}	128.2 ± 6.3^{ad}
	250	263.0 ± 8.2	229.7 ± 9.1^{c}	173.9 ± 8.7^{ac}	125.8 ± 5.0^{ad}
P5	100	270.1 ± 8.8	222.1 ± 7.3^{c}	165.8 ± 6.5^{ac}	131.4 ± 4.7^{a}
	250	265.6 ± 7.7	212.9 ± 7.0^{c}	158.8 ± 5.6^{ac}	128.1 ± 8.0^{a}

All the values are given as mean ± SEM; n = 5; Diabetic control vs all group ([a]p<0.01, [b]p< 0.05), Normal control vs all group ([c]p<0.01, [d]p<0.05)

Table IV					
Effect on body weight of the synthesized compounds					
Group	Dose (mg/kg,p.o)	0 day	5th day	10th day	15th day
Normal control	0.3% CMC	190.6 ± 2.8	191.6 ± 2.8	192.6 ± 2.8	195.6 ± 2.4
Diabetic control		182.4 ± 1.5	181.2 ± 1.6	176.6 ± 2.3	184.4 ± 2.2
Standard (miglitol)	25	148.1 ± 8.4	146.1 ± 8.3^{ac}	142.4 ± 8.1^{ac}	134.4 ± 9.3^{ac}
P22	100	147.7 ± 8.7^{a}	146.2 ± 8.8^{ac}	144.2 ± 8.2^{ac}	142.7 ± 8.1^{ac}
	250	142.4 ± 7.4^{a}	140.6 ± 7.5^{ac}	138.3 ± 7.4^{ac}	136.8 ± 7.2^{ac}
P10	100	143.6 ± 8.7^{a}	141.6 ± 8.3^{ac}	140.1 ± 8.0^{ac}	138.7 ± 8.0^{ac}
	250	144.5 ± 6.7^{a}	141.5 ± 6.8^{ac}	139.4 ± 6.4^{ac}	138.3 ± 6.4^{ac}
P2	100	141.3 ± 4.4^{a}	140.1 ± 4.5^{ac}	137.6 ± 4.6^{ac}	136.2 ± 4.6^{ac}
	250	140.3 ± 4.4^{a}	138.2 ± 4.7^{ac}	135.7 ± 4.9^{ac}	134.0 ± 5.0^{ac}
P4	100	135.5 ± 4.3^{a}	132.7 ± 4.2^{ac}	130.1 ± 4.3^{ac}	128.2 ± 4.0^{ac}
	250	140.5 ± 9.0^{a}	137.6 ± 8.7^{ac}	135.5 ± 8.4^{ac}	133.4 ± 8.1^{ac}
P5	100	140.2 ± 6.7^{a}	138.5 ± 6.6^{ac}	136.8 ± 6.4^{ac}	135.3 ± 6.4^{ac}
	250	140.3 ± 6.5^{a}	138.2 ± 7.1^{ac}	136.0 ± 7.2^{ac}	133.8 ± 7.4^{ac}

All the values are given as mean ± SEM; n = 5; Diabetic control vs all group ([a]p<0.01, [b]p< 0.05), Normal control vs all group ([c]p<0.01, [d]p<0.05)

control group. Effects of drugs over body weight and the changes in body weight after two weeks of treatment were given in the Table IV.

Effect on SGOT, SGPT, ALP, TC and TG level

Activity of the enzymes SGOT, SGPT and ALP were measured from the plasma of the experimental animals. The level of TC and TG content was also measured from the plasma collected from the rats after 14 days treatment using biochemical kits and results are represented in Table V.

Elevation of biomarker enzymes such as SGOT, SGPT ALP were observed in diabetic group which indicates hepatic damage. On treatment with synthesized compounds reduced the levels of the elevated marker enzymes i.e. SGOT, SGPT, ALP and restored these close to normal values which indicates recovery of insulin secretion. So it can be clearly understood that there is positive effect which is statistically significant (p<0.01).

Table V						
Effect on SGOT, SGPT, ALP, TC and TG levels						
Group	Dose level (mg/kg,p.o)	SGOT (mg/dL)	SGPT (mg/dL)	ALP (mg/dL)	Total choles-terol (mg/dL)	Triglyceride (mg/dL)
Normal control	0.3% CMC	72.3 ± 2.1	76.7 ± 2.2	135.6 ± 2.3	132.6 ± 5.4	113.2 ± 4.6
Diabetic control		139.9 ± 3.4	167.3 ± 1.3	230.2 ± 1.3	267.2 ± 1.1	214.1 ± 1.0
Standard (miglitol)	25	81.9 ± 2.4[ab]	89.2 ± 3.8[ad]	158.2 ± 4.9[ac]	183.1 ± 2.5[ac]	138.4 ± 5.4[ac]
P22	100	107.5 ± 4.5[ab]	116.8 ± 6.6[ac]	177.9 ± 5.5[ac]	197.5 ± 3.54[ac]	154.6 ± 2.23[ac]
	250	115.56 ± 3.7[ac]	116.77 ± 7.1[ac]	192.2 ± 4.6[ac]	203.9 ± 7.9[ac]	158.6 ± 4.5[ac]
P10	100	104.6 ± 4.2[ac]	113.4 ± 6.1[ac]	186.1 ± 5.5[ac]	190.6 ± 2.3[ac]	152.3 ± 3.3[ac]
	250	115.9 ± 2.6[ac]	125.6 ± 10.7[ac]	199.0 ± 12.8[bc]	195.5 ± 3.4[ac]	160.2 ± 6.4[ac]
P2	100	95.2 ± 2.7[ac]	108.4 ± 3.3[ac]	179.8 ± 6.2[ac]	201.0 ± 2.5[ac]	151.1 ± 3.6[ac]
	250	106.8 ± 3.0[ac]	127.2 ± 2.7[ac]	195.8 ± 3.3[ac]	194.3 ± 4.0[ac]	153.2 ±9.0[ac]
P4	100	91.2 ± 2.5[ac]	107.2 ± 1.0[ac]	172.9 ± 6.3[ac]	189.5 ± 2.2[ac]	148.9 ± 4.4[ac]
	250	103.8 ± 2.9[ac]	127.5 ± 3.5[ab]	198.5 ± 3.2[bc]	198.7 ± 5.9[ac]	151.3 ± 1.2[ac]
P5	100	85.3 ± 3.6[ad]	110.6 ± 2.7[ab]	181.8 ± 4.8[ac]	191.3 ± 8.7[ac]	154.2 ± 2.2[ac]
	250	99.9 ± 0.9[ac]	125.5 ± 6.3[ab]	188.6 ± 8.2[ac]	201.5 ± 7.7[ac]	157.5 ± 3.4[ac]

Diabetic control vs all group ([a]p<0.01, [b]p< 0.05), Normal control vs all group ([c]p<0.01, [d]p<0.05)

Discussion

Type 2 diabetes mellitus is major health problem. In this manuscript we present an approach to control blood glucose levels in individuals with type 2 diabetes by targeting maltase-glucoamylase and intestinal glucosi-dases using some novel xanthone alpha-glucosidase inhibitors. One of the intestinal glucosidases targeted the N-terminal catalytic domain of maltase-gluco-amylase (ntMGAM) which is responsible for the hydro-lysis of terminal starch products into glucose (Sim et al., 2010). Hence to slow down the glucose level we targeted the ntMGAM. Previously acarbose and migli-tol were found to be potent inhibitors alpha-glucosidase having polyhydroxy groups in their structure (Asano et al., 2003). Hence novel molecules are designed to xanthone based on the fact. Computational docking study was done to the binding pocket of miglitol with the crystal structure of maltase-glucoamylase. We re-docked to verify the interaction of the cocrystal ligand (miglitol) with the novel xanthone molecules. We obser-ved excellent correlation in docking. Based on the docking interaction we synthesized the most effective compounds. *In vivo* acute toxicity study showed the synthesized compounds showed no serious toxicity up to dose level 1500 mg/kg body weight in experimental rats. The molecules were screened for the *in vivo* anti-diabetic activity in streptozotocin-induced diabetic animal model. After 72 hours of STZ treatment the blood glucose level was significantly changed more than 240 mg/dL. Statistical analysis by one way ANOVA revealed that there was significant decrease

(p<0.01) in blood glucose level of the animals after treat-ment with drugs on 5th day, 10th day and 15th day.

The designed ligands were predicted for bioavailability and others molecular property to check their potential as future drug candidate and they hardly violating those filters. When they docked in the same binding pocket with same amino acid residues of targeted protein most of the derived ligands predicted better binding energy than miglitol. Among 28 designed compounds the compound p22 showed to have the best binding energy (-12.99 Kcal/mol) however the compound p26 showed the least binding energy (-7.17 Kcal/mol). Based on these i*n silico* results further proceded for the laboratory experiment. Top five compounds were synthesized in laboratory scale, purified and crystallized properly to characterize them by UV, FTIR, NMR and mass analysis. The analytical and spectral data of the compounds analyzed and are found in compliance with the structure of the synthesized compounds.

The compounds were further screened for *in vivo* anti-diabetic activity using streptozotocin-induced diabetic model in Wistar rats. Effective dose was selected after oral acute toxicity study. All the study group animals were subjected to 15 days anti-diabetic treatment proto-col and blood glucose level were measured on 0th, 5th, 10th and 15th day collecting blood from tail vein of study subjects. Study shows a significant reduction in blood glucose as well as it was also noted that the total cholesterol and triglycerides level was increased in diabetic control groups and there was a notable change

after 15 days treatment with synthesized compounds. On treatment with synthesized compounds total cholesterol and triglyceride level decreased significantly (p<0.01) as compared with diabetic control group.

Conclusion

Xanthone derivatives proved to act as lead molecules towards the development of potential α-glucosidase inhibitors. These compounds showed excellent correlation between docking results, synthetic data and *in-vivo* anti-diabetic activity.

Ethical Issue

Anti-diabetic activity evaluation was performed after the approval (IEAC/DU/57 dated 24.9.2013) of Institutional animal Ethical Committee of laboratory animals of Department of Pharmaceutical Sciences, Dibrugarh University, Assam, India (Regd. No. 1576/GO/a/11/CPCSEA dated 17/2/2012).

Conflict of Interest

The authors declare that they have no competing interests.

Acknowledgement

References

Abeeleh ME, Ismail ZB, Khaled R, Sami AHA, Mohamed AEK, Abuabeeleh J, Alsmady MM. Induction of diabetes mellitus in rats using intraperitoneal streptozotocin: A Comparison between 2 strains of rats. Eur J Sci Res. 2009; 32: 398-402.

Asano N. Glycosidase inhibitors: Update and perspectives on practical use. Glycobiology. 2003; 13: 93104.

Campbell, LK, Baker DE, Campbell RK. Miglitol: Assessment of its role in the treatment of patients with diabetes mellitus. Ann Pharmacother. 2000; 34: 1291-301.

Cardona ML, Fernandez MI, Pedro JR, Serrano A. Xanthones from hypericum reflexum. Phytochemistry. 1990; 29: 3003-6.

Cole JC, Murray CW, Nissink, JWM, Taylor RD, Taylor R. Comparing protein-ligand docking programs is difficult. Proteins, 2005; 60: 325–32.

Diderot NT, Silvere N, Etienne T. Xanthone as therapeutic agents. Chem Pharmacol. 2006; 2: 273-98.

Du Z-Y, Liu R-R, Shao W-Y, Mao XP, Ma L, Gu L-Q, Huangm Z-S, Chan ASC. Alpha-glucosidase inhibition of natural

curcuminoids and curcumin analogs. Eur J Med Chem. 2006; 41: 213-18.

Eaton PE and Carlson GR. Phosphorous pentoxide-methanesulfonic acid. Convenient alternative to polyphosphoric acid. J Org Chem. 1973; 38: 4071-73.

Galt RH, Horbury J, Matusiak ZS, Pearce RJ, Shaw JS. Thexanthene-9-spiro-4′-piperidine nucleus as a probe for opiate activity. J Med Chem. 1989; 32: 2357-62.

Heightman, TD, Andrea T, Vasella AT. Recent insights into inhibition, structure, and mechanism of configuration-retaining glycosidases. Angew Chem Int Ed. 1999; 38: 750-70.

Hsiao SH, Liao LH, Cheng PN, Wu TJ. Hepatotoxicity associated with acarbose therapy. Ann Pharmacother. 2006; 40: 151–54.

Humphries MJ, Matsumoto K, White SL, Olden K. Inhibition of experimental metastasis by castanospermine in mice: Blockage of two distinct stages of tumor colonization by oligosaccharide processing inhibitors. Cancer Res. 1986; 46: 5215-22.

Karpas A, Fleet GW, Dwek RA, Petursson S, Namgoong SK, Ramsden NG, Jacob GS, Rademacher TW. Aminosugar derivatives as potential anti-human immunodeficiency virus agents. Proc Natl Acad Sci USA. 1988; 85: 9229-33.

Konc J, Konc JT, Penca M, Janezic M. Binding-sites prediction assisting protein-protein docking. Acta Chim Solv. 2011; 58: 396-401.

Kumudhavalli MV and Jaykar B. Evaluation of anti-diabetic activity of Costus igneus(L) leaves on STZ induced diabetic rats. Der Pharmacia Sinica, 2012; 3: 1-4.

Liu Y, Ma L, Chen W-H, Wang B, Xu Z-L. Synthesis of xanthone derivatives with extended π-systems as a-glucosidase inhibitors– insight into the probable binding mode. Bioorg Med Chem. 2007; 15: 2810-14.

Liu Y, Zou L, Ma L, Chen W-H, Wang B, Xu ZL. Synthesis and pharmacological activities of xanthone derivatives as a-glucosidase inhibitors. Bioorg Med Chem. 2006; 14: 5683–90.

Luo J-G, Wang X-B, Ma L, Kong L-Y. Gypsophin: A novel alpha-glucosidase inhibitory cyclic peptide from the roots of Gypsophila oldhamiana. Bioorg Med Chem Lett. 2007; 17: 4460-63.

Madeswaran A, Umamaheswari M, Asokkumar K, Sivashanmugam T, Subhadradevim V, Jagannath P. *In silico* docking evaluation of α-Amylase inhibitory activity of butein and tricetin. J Comput Method Mol Design. 2011; 14: 65-72.

Mehta A, Zitzmann N, Rudd PM, Block TM, Dwek RA. Alpha-glucosidase inhibitors as potential broad based anti-viral agents. FEBS Lett. 1998; 430: 17-22.

Morris GM, Goodsell DS, Halliday RS, Huey R, Hart WE, Belew RK, Olson AJ. Xanthones from hypericum reflexum automated docking using a lamarckian genetic algorithm and and empirical binding free energy function. J Comput Chem. 1998; 19: 1639-62.

Nainwal LM, Parida P, Das A, Bairy PS. Design and docking of novel series of hybrid xanthones as anticancer agent to target human DNA topoisomerase 2-alpha. Bangladesh J

Pharmacol. 2014; 9: 204-17.

Park JH, Ko S, Park H. Toward the Virtual Screening of α-Glucosidase Inhibitors with the Homology-Modeled Protein Structure. Bull Korean Chem Soc. 2008; 29: 921-27.

Pickert M, Schaper KJ, Frahm AW. Substituted xanthones as antimycobacterial agents. Part 2: Antimycobacterial activity. Arch Pharm (Weinheim). 1998; 331; 193-97.

Ramachandan S, Rajasekaran A, Adhirajan N. *In vivo* and *in vitro* anti-diabetic activity of *Terminalia paniculata* bark: An evaluation of possible phytoconstituents and mechanisms for blood glucose control in diabetes. ISRN Pharmacology. 2013; 2013: 1-10.

Saludes JP, Lievens SC, Molinski TF. Occurrence of the alpha-glucosidase inhibitor 1,4-Dideoxy-1,4-imino-D-arabinitol and related iminopentitols in marine sponges. J Nat Prod. 2007; 70: 436-38.

Selvan VT, Manikandan L, Senthil KGP. Anti-diabetic and Anti-oxidant effect of methanol extract of *Artanema sesamoides* in streptozotocin-induced diabetic rats. Int. J App Res Nat Prod. 2008; 1: 25-33.

Silverstein RM and Webster FX. Spectrometric identification of organic compounds. John Wiley and Sons Ltd., 1963; New York.

Sim L, Jayakanthan K, Mohan S, Nasi R, Johnston BD, Pinto BM, David RR. New glucosidase inhibitors from an Ayurvedic herbal treatment for type 2 diabetes: Structures and inhibition of human intestinal maltase-glucoamylase with compounds from salacia reticulata. Biochemistry 2010; 49: 443–51.

Tanabe G, Yoshikai K, Hatanaka T, Yamamoto M, Shao Y, Minematsu T, Muraoka O, Wang T, Matsuda H, Yoshikawa M. Biological evaluation of de-O-sulfonated analogs of salacinol, the role of sulfate anion in the side chain on the α-glucosidase inhibitory activity. Bioorg Med Chem. 2007; 15: 3926-37.

Varache-Lembege M, Moreau S, Larrouture S, Montaudon D, Robert J, Nuhrich A. Synthesis and anti-proliferative activity of aryl- and heteroaryl-hydrazones derived from xanthone carbaldehydes. Eur J Med Chem. 2008; 43: 1336-43.

Xu H-W, Dai G-F, Liu G-Z, Wang J-F, Liu H-M. Synthesis of andrographolide derivatives: A new family of alpha-glucosidase inhibitors. Bioorg Med Chem. 2007; 15: 4247-55.

Zitzmann N, Mehta AS, Carrouee S, Butters TD, Platt FM, McCauley J, Blumberg BS, Dwek RA, Block TM. Imino sugars inhibit the formation and secretion of bovine viral diarrhea virus, a pestivirus model of hepatitis C virus: Implications for the development of broad spectrum anti-hepatitis virus agents. Proc Natl Acad Sci USA. 1999; 96: 11878-82.

Author Info
Pratap Parida (Principal contact)
e-mail: pratapparida2007yahoo.com@gmail.com

Your feedback about this paper

1. Number of times you have read this paper

2. Quality of paper

3. Your comments